Journal of Power Sources 185 (2008) 932–936

Contents lists available at ScienceDirect

Journal of Power Sources

journal homepage: www.elsevier.com/locate/jpowsour

Short communication

Cathode contact optimization and performance evaluation of intermediate temperature-operating solid oxide fuel cell stacks based on anode-supported planar cells with $LaNi_{0.6}Fe_{0.4}O_3$ cathode

Satoshi Sugita*, Yoshiteru Yoshida, Himeko Orui, Kazuhiko Nozawa, Masayasu Arakawa, Hajime Arai

NTT Energy and Environmental systems Laboratories, NTT Corporation, 3-1, Morinosato-Wakamiya, Atsugi-shi, Kanagawa 243-0198, Japan

ARTICLE INFO

Article history:
Received 31 March 2008
Received in revised form 14 July 2008
Accepted 16 July 2008
Available online 3 August 2008

Keywords:
SOFC
Stack
Anode-supported
Metallic separator
Cathode contact

ABSTRACT

This paper reports the development of intermediate temperature-operating solid oxide fuel cell stacks using anode-supported planar cells with $LaNi_{0.6}Fe_{0.4}O_3$ (LNF)cathode. We developed metallic separators with radial gas flow channels and an anode seal structure. To achieve good power-generating characteristics, we propose two cathode contact methods. According to a performance evaluation at 800 °C, power density of 0.5 W cm^{-2} is obtained at the current density of 1.0 A cm^{-2} when operating with a sufficient fuel amount, and power conversion efficiency of over 50% LHV is obtained at the current density of more than 0.2 A cm^{-2} when operating at a high fuel utilization rate.

1. Introduction

Recently, solid oxide fuel cells (SOFCs) have received more attention because of their high efficiency, high heat utilization and good fuel flexibility. Nevertheless, a number of issues must be solved before SOFCs can be applied to an actual power system [1–3].

Currently, there are two basic designs for SOFC application: planar and tubular [1,3–7]. Planar cell designs are expected to be cost-effective, and mechanically robust, and to offer higher power density per unit volume [5–7].

To realize a SOFC system that has high power generation efficiency (or high electrical conversion efficiency) using planar type cells, there are two important points.

One is that the cell operating voltage should be as high as possible under certain current density and fuel utilization conditions. Here, the intrinsic cell performance and electrical contact between the cell and separators are the most important factors.

The other is that the performance of the cell-separator system, which includes the separator structure, gas flow pattern and sealing method, should be optimized so as to achieve high fuel utilization under the desirable current density condition.

On the other hand, for an actual SOFC system, there are practical demands regarding reliability, durability and cost competitiveness.

To meet these practical requirements, there are certainly constraints for the cell operating voltage and fuel utilization rate, which greatly depend on the type of structure and the scales of the SOFC stacks.

In our previous work, we have successfully fabricated anode-supported cells that operate at below 800 °C by co-sintering of anode substrate and scandia- and alumina-stabilized zirconia (SASZ) electrolyte. [8–10] $LaNi_{0.6}Fe_{0.4}O_3$ (LNF) was applied to our anode supported cell. We have confirmed that the cells with LNF cathode have both high electrochemical performance even at 800 °C [11,12] and chemical stability against chromium species that comes from the metallic separators used in the SOFC stack [13].

In this paper, we describe the design and fabrication of the metallic separators for our anode-supported SOFCs and their performance. To achieve high electrical conversion efficiency of over 50%, we set our target as an operating cell voltage of 0.8 V at a fuel utilization rate of over 70% under reasonable current density conditions.

We discuss the current–voltage (I–V) characteristics and fuel utilization properties of the cell-separator system, and address the key issue in realizing high performance with respect to the cathode contact method.

* Corresponding author. Tel.: +81 422 592913; fax: +81 422 595600.
E-mail address: sugita.satoshi@lab.ntt.co.jp (S. Sugita).

0378-7753/$ – see front matter © 2008 Elsevier B.V. All rights reserved.
doi:10.1016/j.jpowsour.2008.07.072

2. Experimental

2.1. Cell

In our previous work [8–13], high performance disk shaped anode-supported SOFCs with LNF cathode were developed. The electrolyte was 10 mol % Sc_2O_3- and 1 mol % Al_2O_3-stabilized ZrO_2 (SASZ, Daiichi Kigenso Kagaku Kogyo Co.). The anode was a mixture of 60 wt% NiO and 40 wt% SASZ. The anode and electrolyte green sheets were prepared by the doctor blade method. The anode green sheets were laminated to obtain appropriate thickness of about 1 mm. The electrolyte green sheet was laminated on the anode green sheets. These laminated sheets were cut into disks and co-sintered at 1350 °C to make half cells. The cathode was $LaNi_{0.6}Fe_{0.4}O_3$ (LNF). Slurry of LNF was screen-printed on the electrolyte of the half cell and sintered. The details of the cell fabrication process are described elsewhere [10–12]. In this report, cells of 60 mm-diameters were used.

2.2. Power generating test using Pt current collector and alumina housing

Electrochemical measurements on the fabricated cell were performed by using alumina housing and platinum current collectors [12]. Pt-mesh with Pt voltage probe and Pt current lead were sintered onto each electrode of the cell at 1000 °C for 2 h before power generating tests. The cell was set in the alumina housing with gas manifolds to feed fuel and air, and sealed at the outer edge with glass powder paste. Gas flow channels of the alumina housing for fuel and oxidant gases were designed to induce a radial flow from the center of the cell to the edge. Power-generating tests were conducted while the alumina housing was placed in electrical furnace of 800 °C. The *I–V* characteristics were measured at the condition of 500 mL min^{-1} of dry H_2 and 1.0 L min^{-1} of air for fuel and oxidant gases, respectively.

Fig. 1 shows a photograph of the cell with the Pt current collector in the alumina housing.

2.3. Separator structure and sealing

Fig. 2 shows a cross-sectional illustration of our metal separator system.

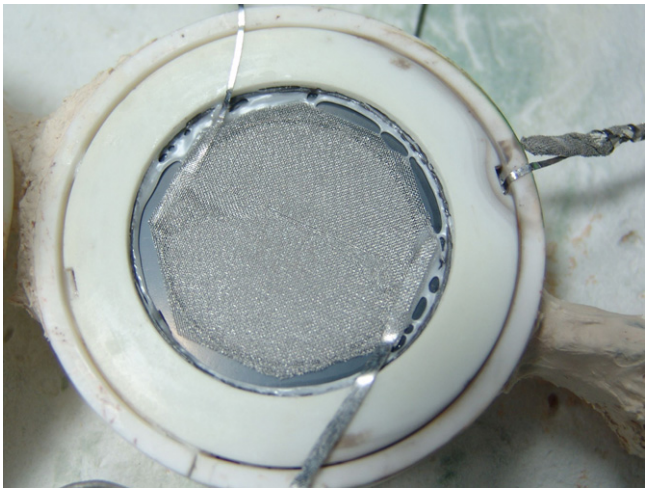

Fig. 1. Photograph of the Pt current collector sintered on the cathode. The cell is in an alumina housing.

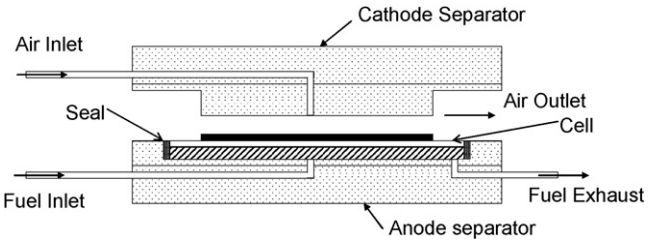

Fig. 2. Cross-sectional illustration of our cell-separator system for the planar anode-supported cell.

A chamber is placed at the center of the anode-separator and set the anode-supported cell in it. Sealing was made between cell and anode separator at the outer edge of the disk shaped cell. The sealant was a mixture of ceramic fiber and glass powder paste. The cathode separator is designed to touch the cell only in the cathode electrode area of the cell. External pressure to this area was controlled by using a press rod from outside the furnace. Fig. 3 is a photograph of our anode separator. The gas flow channels of the separator system for fuel and oxidant gases were designed to induce a radial flow from center of the cell to the edge.

2.4. Cathode contact layer

In this study, we tested three cathode-separator contact methods: The separator directly contacting the cathode of the cell; Pt-paste and a mat of non-woven stainless steel wire (SUS-mat) placed between the separator and the cathode; and ceramic powder paste of LNF, which is the same material as the cathode of the cell, placed between the separator and the cathode and sintered just before power generating test at 800 °C.

Fig. 4(a)–(c) are photographs of direct contact method, SUS-mat and Pt-paste method, LNF-paste method, respectively.

For all contact methods, mechanical load was added to the cathode separator to make the contact firmer.

2.5. Power-generating test and AC impedance measurement for cell-separator system

Power-generating tests were conducted while the cell-separator system described above was set in an electrical furnace of 800 °C. *I–V* characteristics were measured at the condition of 300 mL min^{-1}

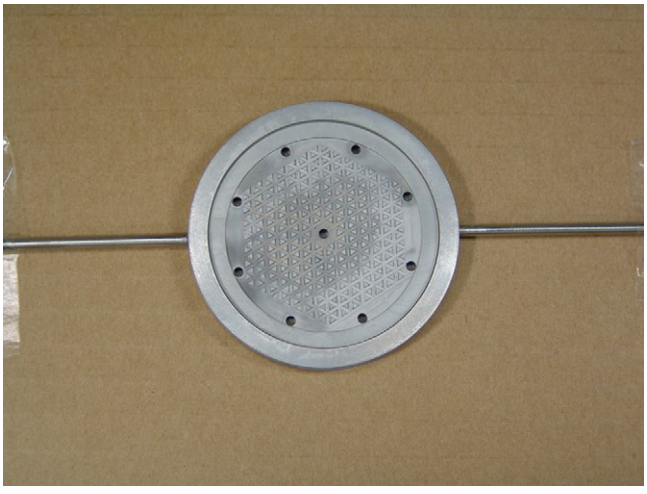

Fig. 3. Our anode-side metallic separator for a 60-mm anode supported cell.

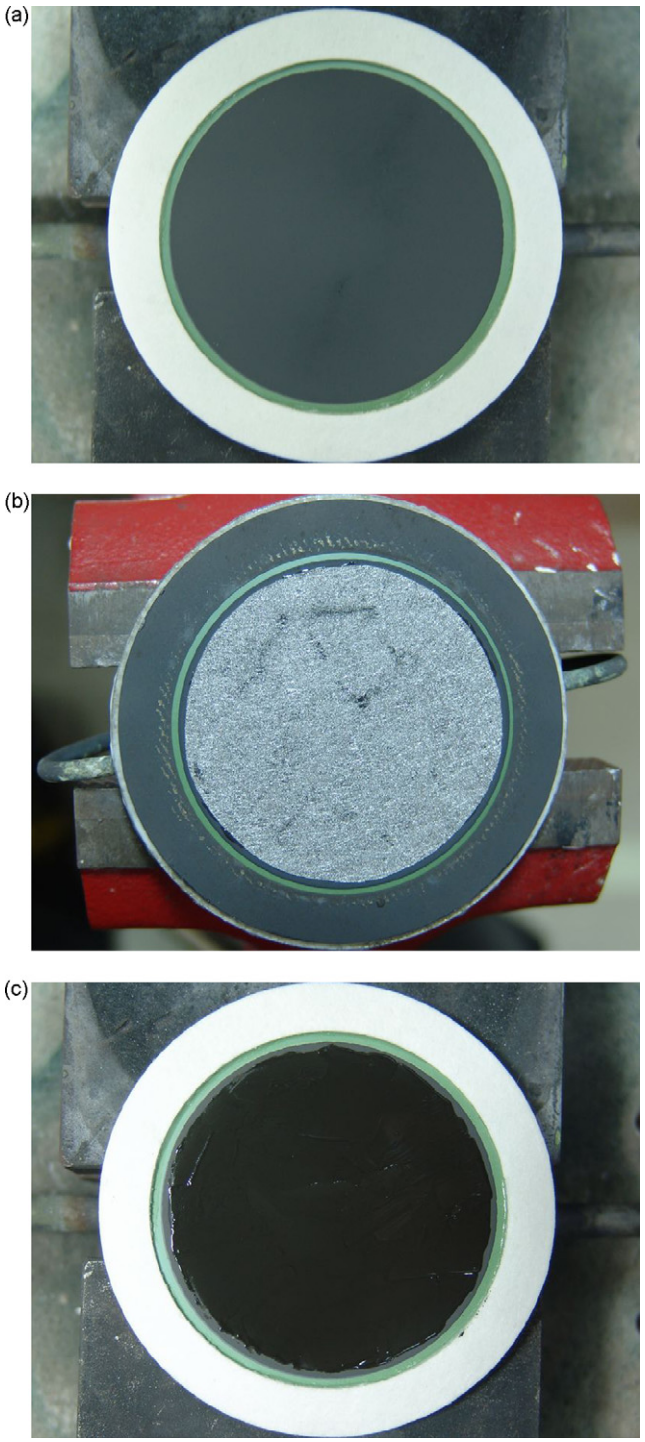

Fig. 4. Photographs of cathode contact methods. (a) No contact layer on the cathode (direct contact). (b) SUS-mat and Pt-paste placed on the cathode. (c) LNF-paste applied on the cathode.

of dry H_2 and 1.0 L min^{-1} of air for fuel and oxidant gases, respectively. For measurements of fuel utilization dependence, cell voltages of fixed current load were measured while changing the fuel flow rate. Internal resistances of cell-separator systems were investigated by the AC impedance method. The measurements were carried out at the open circuit voltage (OCV) at frequencies ranging from 10 mHz to 100 kHz using a Solatron 1260 impedance analyzer.

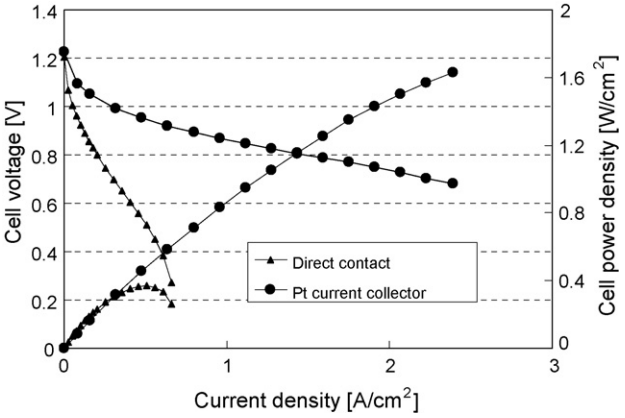

Fig. 5. *I–V* characteristics of our anode-support cells. The circles and triangles indicate data measured using the alumina-housing with the Pt-current collector and those measured using the metal separator direct-contact method, respectively.

3. Results and discussion

3.1. Direct contact

I–V and current-power characteristics of our anode-support cells are shown in Fig. 5 for two test configurations: alumina housing with the Pt-current collector (Pt-mesh method) and metal-separator in the direct contact method. With the Pt-mesh method, a large power output of 1.6 W cm^{-2} was obtained. We assume that this is an intrinsic characteristic of the cell itself. It is clear from the results shown in Fig. 5 that using a metal separator and just having it contact the cathode directly cannot bring enough power that the cell originally has.

Fig. 6 shows Cole–Cole plots of the AC impedance spectra of these two conditions. The internal resistance of the cell/cell-separator system can be separated into three parts from the Cole–Cole plot of AC impedance spectra: R0, which is the intersection point of real part axis, and R1 and R2, which were obtained from the diameter of the semicircles appearing in the high-frequency part and low-frequency part, respectively. The intersection point (R0) reflects an ohmic resistance of the cell/cell-separator system.

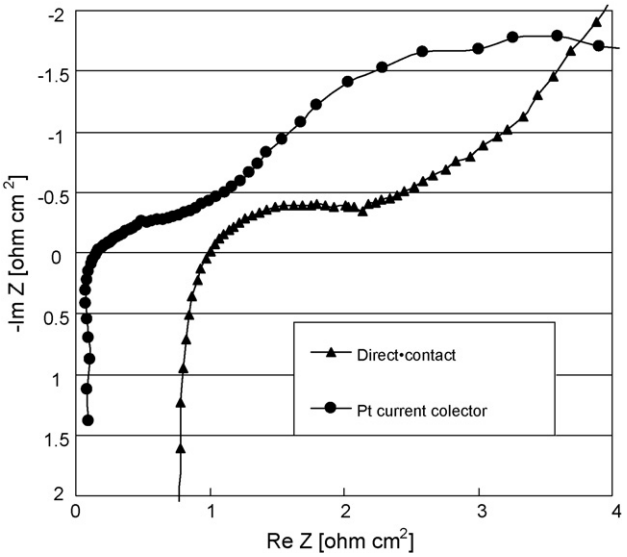

Fig. 6. Comparison of AC impedance spectra. The circles and triangles indicate data measured using the alumina-housing with the Pt-current collector and those measured using the metal separator direct-contact method, respectively.

We identified the high-frequency semicircle (R1) as a cathodic reaction [11]. And, we think that the low frequency part (R2) is related to the anodic reaction because its measured value changes depending on the flow rate of the fuel and/or the species of the fuel. For an accurate measurement of this R2 component, it is indispensable to measure under the fuel condition that the oxygen partial pressure of anode side does not change heavily by the electrical current applied for the measurement. For example, measurements under humidified hydrogen fuel condition or under certain discharged condition (for our measurements, under the condition of at least 0.2 A cm^{-2} to 0.3 A cm^{-2}) are needed. However, such a condition was not able to be prepared in our measurement environment. So, it is not appropriate to discuss about this R2 components in the data shown here. But, we confirmed that the R0 values were not affected by the fuel condition discussed above. In this paper, we discuss about the relation between the measured value of R0 and the method of cell separator contact method.

The apparent difference between these two cases is the magnitude of R0: R0 = 0.16 Ω cm^2 for the Pt-mesh method and 0.97 Ω cm^2 for the metal separator. This indicates that the large R0 value greatly degrades the cell power output under the direct contact condition, and that reduction of this contact resistance, possibly without using costly noble metal materials, is required.

3.2. Influence of cathode contact layer

To reduce contact resistance between the metallic separator and cathode, we tested the contact method with the Pt-paste and SUS-mat placed between the separator and cathode and the one with ceramic powder paste of LNF placed between the separator and cathode.

We expected that the former method would show the same performance as the alumina-housing measurement in that both use Pt-paste and metal mat to collect current.

The latter method is aimed at filling the space between cathode and contact area of metallic separator by the LNF powder. This LNF powder is the same powder used for the cathode. Only the sintering temperature is different between the cathode and contact paste.

Fig. 7 shows the *I–V* and current-power characteristics for these two cathode contact methods. The data for the direct contact method are also shown for comparison. These two shows nearly the same performances, and the performance is relatively high compared to direct contact. And their AC impedance results (Fig. 8) also indicate almost same R0 value of R0 = 0.33 Ω cm^2.

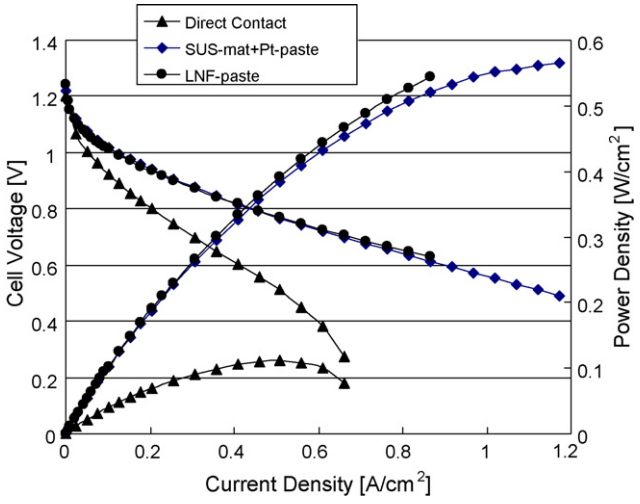

Fig. 7. *I–V* characteristics of our anode-support cells with two cathode contact methods. The diamonds and circles indicate data measured using the SUS-mat and Pt-paste contact layer and those measured using the LNF-paste contact layer, respectively. For comparison, data for the direct-contact method (triangles) are re-plotted from Fig. 5.

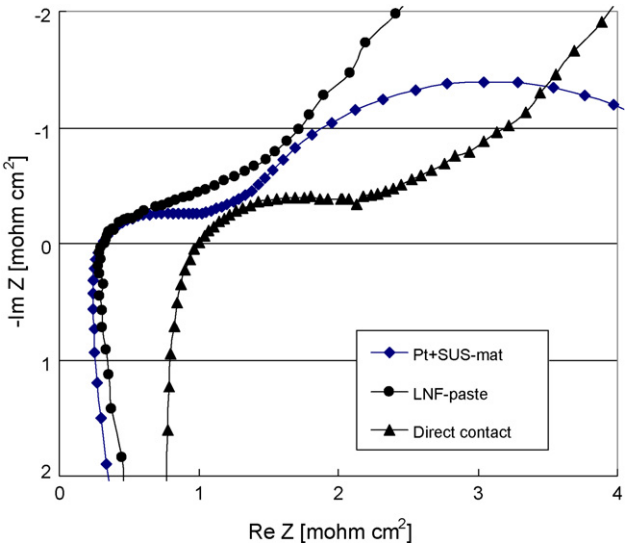

Fig. 8. Comparison of AC impedance spectra for two cathode contact methods. The diamonds and circles indicate data measured using the SUS-mat and the Pt-paste contact layer and those measured using the LNF-paste contact layer, respectively. For comparison, data for the direct-contact method (triangles) are re-plotted from Fig. 6.

These two contact methods reduce ohmic resistance between cathode and metallic separator and improve current–voltage characteristics significantly. But the contact resistance of these two cases is still larger than that for the Pt-mesh method.

A possible reason for the insufficient contact is that the metallic separator surface and the current collector (or the cell) were both so rigid that there were only point-to-point connections between them. We expect that further improvement would be possible by optimizing the cathode contact layer. Nevertheless, reasonable cell voltage of 0.8 V was achieved in this experiment at the current density of 0.4 A cm^{-2}, when the fuel amount was sufficient.

3.3. Fuel utilization dependence

Fig. 9 shows the fuel utilization dependence of the cell voltage of our cell-separator system. The cathode contact method of Pt-paste and SUS-mat was used for this measurement. To obtain the fuel utilization dependence, cell voltages were measured while the fuel flow rate was changed at each current set point. From the results, it is clear that our cell-separator system can be operated without any failure or degradations up to the fuel utilization of more than 80%. This, together with the *I–V* characteristics above, suggest that our cell-separator system has sufficient performance to realize the SOFC stack with high power conversion efficiency of over 50% LHV at the current density of up to 0.2 A cm^{-2}.

We think that such a stable power generation performance at the condition of high fuel utilization rate and high power conversion efficiency are achieved mainly by two reasons. One is the good *I–V* characteristics due to the good cell performance and the good cathode contact. The other is the tolerance against severe operating condition such as high fuel utilization rate resulting from the sealing method and separator structure, especially for disk shaped cell and radial flow gas channels.

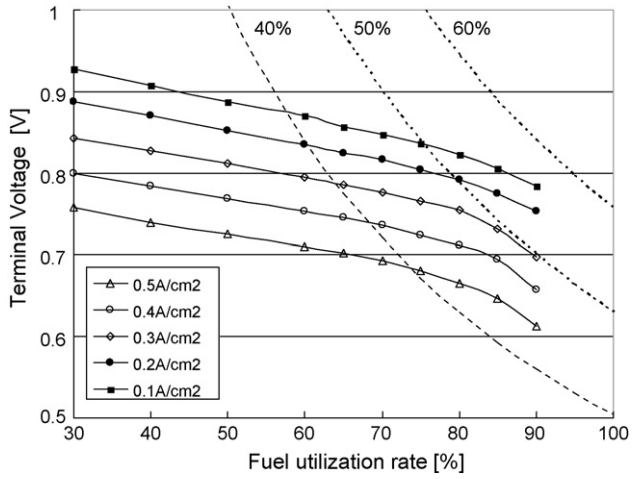

Fig. 9. Fuel utilization dependence of the cell voltage of our cell-separator system with the SUS-mat and Pt-paste cathode contact layer. Current load of the cell was set at the current density of 0.1, 0.2, 0.3, 0.4, or 0.5 A cm^{-2}. The dashed lines indicate the contour of power conversion efficiency for 40%, 50%, and 60%.

For the case of square cell, it is not easy to make radial gas flow channels on the separators. For example, Borglum et al. used separators with parallel gas channels and placed gas inlets at one side of a cell [6]. In this case, operation at high fuel utilization rate is strongly affected by sealing performance because fresh fuel may cross the seal part at the boundary between the cell and the separator.

Further studies are needed to clarify the influences of stack design such as cell shape, gas flow pattern, and sealing performance to power generation performance. But we think that our disk shaped cell and separator with radial gas flow from the center of the cell have advantages for realizing high fuel utilization operation.

4. Conclusion

A disk shaped planar-type cell-separator system with radial gas flow and anode sealing structure was presented. The system was assembled using a 60-mm anode-supported cell with LNF cathode and glass-ceramics mixture sealant. Its electrochemical performance is strongly affected by the cathode contact method. As candidate for the cathode contact method, we propose the SUS-mat and Pt-paste contact layer and the LNF paste contact layer. Both methods can improve the performance of the cell-separator system. According to the performance evaluation of our cell-separator system, power density of 0.5 W cm^{-2} are obtained at the current density of 1.0 A cm^{-2} when operating with a sufficient fuel amount and power conversion efficiency of over 50% LHV at the current density of up to 0.2 A cm^{-2} is obtained when operating at a high fuel utilization rate. These results were obtained using hydrogen as a fuel. Higher power conversion efficiency can be expected by using hydrocarbon fuel such as methane.

The performance will be improved by modifying and optimizing the cathode contact method in the future.

References

[1] N.Q. Minh, Journal of the American Ceramic Society 76 (1993) 563.
[2] N.Q. Minh, T. Takahashi, Science and Technology of Ceramic Fuel Cells, Elsevier, Amsterdam, 1995.
[3] S.C. Singhal, K. Kendall, High-Temperature Solid Oxide Fuel Cells: Fundamentals, Design and Applications, Elsevier, Amsterdam, 2003.
[4] S.C. Singhal, Progress in tubular solid oxide fuel cell technology, in: S.C. Singhal, M. Dokiya (Eds.), Proceeding of the Sixth International Symposium on Solid Oxide Fuel Cells (SOFCVI), vol. 99-19, The Electrochemical Society, 1999, pp. 39–51.
[5] F. Nishiwaki, T. Inagaki, J. Kano, J. Akikusa, N. Murakami, K. Hosoi, Journal of Power Sources 157 (2006) 809.
[6] B. Borglum, E. Tang, M. Pastula, J. Kelsall, R. Petri, Proceeding of the 2006 Fuel Cell Seminar, Honolulu, 2006, p. 135.
[7] S. Mukerjee, H. Haltiner, R. Kerr, S. Kelly, S. Shaffer, Proceeding of the 2006 Fuel Cell Seminar, Honolulu, 2006, p. 127.
[8] T. Ishii, Solid State Ionics 78 (1995) 333.
[9] R. Chiba, F. Yoshimura, Y. Sakurai, Solid State Ionics 124 (1998) 281.
[10] K. Nozawa, H. Orui, R. Chiba, M. Arakawa, in: H. Yokokawa, S.C. Singhal (Ed.), Solid Oxide Fuel Cells VII, PV 2001-16, The Electrochemical Society Proceedings series, Pennington, NJ, 2001, p. 983.
[11] H. Orui, K. Watanabe, R. Chiba, M. Arakawa, Journal of Electrochemical Society 151 (9) (2004) A1412.
[12] H. Orui, K. Nozawa, R. Chiba, T. Komatsu, K. Watanabe, S. Sugita, H. Arai, M. Arakawa, ECS Transaction 7 (2007) 255–261.
[13] T. Komatsu, H. Arai, R. Chiba, K. Nozawa, M. Arakawa, K. Sato, Electrochemical and Solid-State Letters 9 (2006) A9.